ACS APPLIED POLYMER MATERIALS

pubs.acs.org/acsapm

Article

Properties of Freeze-Dried Gelatin/Clay Aerogel Composites Crosslinked with Tannic Acid

Lucía G. De la Cruz, Tobias Abt, Noel León, and Miguel Sánchez-Soto*

Cite This: ACS Appl. Polym. Mater. 2023, 5, 7774−7785

Read Online

ACCESS | Metrics & More | Article Recommendations | Supporting Information

ABSTRACT: Polymer-based aerogels are tough, low-density, and thermally insulating materials currently receiving increasing attention. In this work, robust all-natural aerogel composites have been obtained by incorporating nanoscale montmorillonite and tannic acid into a gelatin matrix via freeze-drying. The prepared aerogels exhibited low densities, good compressive properties, and low thermal conductivities. The significant improvement in the thermomechanical properties results from the strong bonding between gelatin and tannic acid. Under fire, the systems exhibited excellent flame retardancy with reduced thermal degradation rate and cone calorimeter burning parameters. A straightforward surface treatment with polydimethylsiloxane gave the aerogels exceptional and durable superhydrophobicity. These multifunctional composite aerogels are considered promising eco-friendly alternatives to synthetic polymer-based foams.

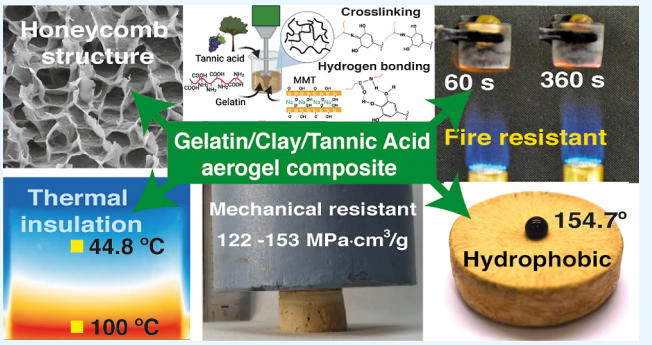

KEYWORDS: *aerogel, gelatin, crosslinking, fire resistance, tannic acid*

1. INTRODUCTION

The current climate emergency requires finding urgent solutions to the environmental problems caused by human activity. Developing highly efficient insulation materials is one approach to save energy and reduce global warming. Synthetic plastic foams based on polyurethane, polystyrene, or phenol−formaldehyde are widely used. However, the pollution caused by non-degradable plastic waste affects the land and the ocean. Increasing concerns about fossil fuel depletion have generated great interest in finding ecological alternatives to these traditional non-renewable petrol-based materials. Among the possibilities, natural and biodegradable polymers have emerged as a logical solution to decrease waste and reduce the environmental impact.[1,2]

Aerogels are lightweight, solid, and open-porous materials obtained from a gel in which the solvent has been replaced by air without collapsing the three-dimensional structure previously created. Their highly porous structure confers aerogels with unique features, such as low density, high specific surface area, and low thermal conductivity, making them useful for various applications, including oil absorption, thermal insulation, and flame retardancy.[3−6] Using polymers of natural origin is one way to create sustainable foamed structures with strong mechanical performance, low thermal conductivity, and fire resistance. Achieving these objectives will facilitate and promote the application of bio-based foam-like materials in sectors such as construction, transport, or packaging.

Gelatin is an inexpensive, biodegradable, water-soluble protein that can be derived from the by-products of various industries. It is usually obtained from the acidic or basic partial hydrolysis of collagen extracted from animal or fish skin, bones, and tissue. The thermal denaturation of collagen produces a high molecular weight protein containing amino acids, glycine, hydroxyproline, and proline linked to each other by peptide bonds. The high number of functional groups in gelatin, including aminos, hydroxyls, and carboxyls, can enhance its properties, for example, through hydrogen bonding or crosslinking. In addition, the presence of significant amounts of nitrogen enables the possibility of using gelatin as a low-flammable material. Mixing gelatin, chitosan, and glycerol, Zhang et al. have created a fully bio-based and self-healing coating suitable for protecting wood against fire.[7] On untreated wood, the coating delayed the ignition time six-fold and decreased the combustion rate by 24% due to the combined action of water cooling, CO_2 release, and char layer formation. Moreover, the reversible hydrogen bond crosslinks between glycerol hydroxyls, chitosan, and gelatin chains gave the coatings a self-healing ability. Despite the flame-retardant

Received: May 10, 2023
Accepted: August 18, 2023
Published: September 10, 2023

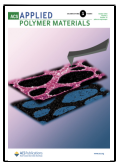

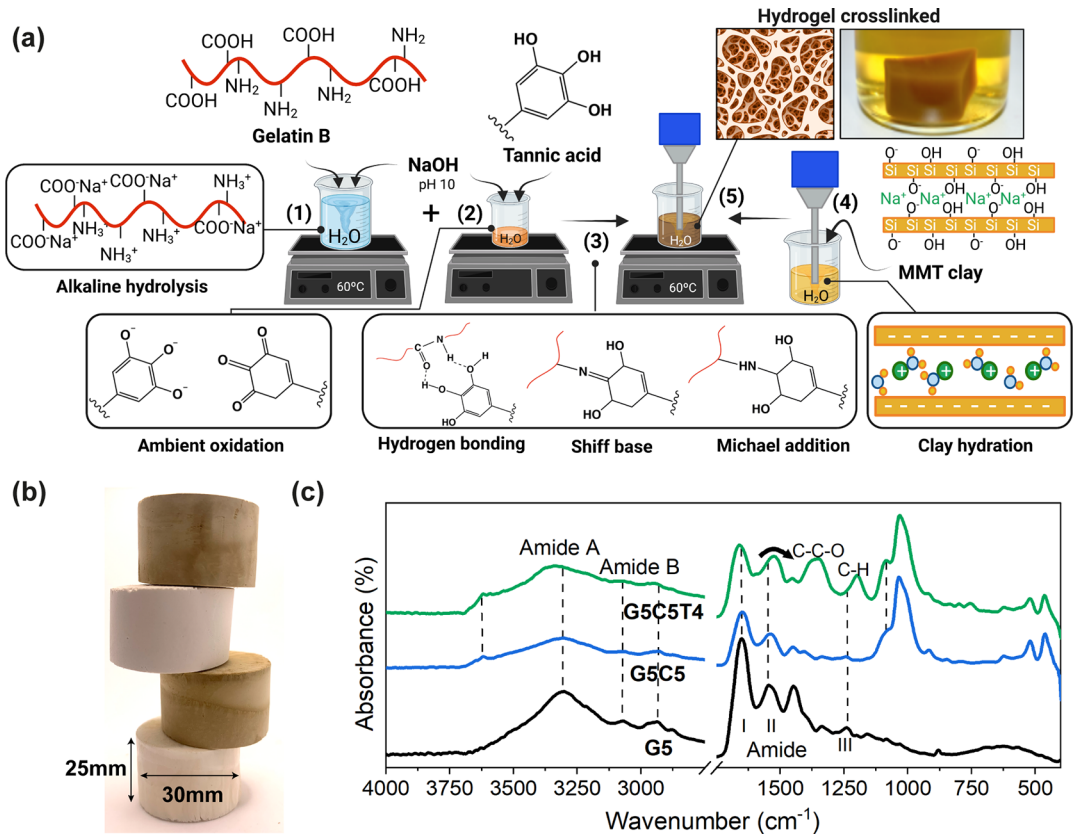

Figure 1. (a) Aerogel preparation and proposed reaction mechanism (created with Biorender.com Agrmt. no. PT25NOG1DC), (b) aerogel monolith photographs, and (c) FTIR spectra of representative aerogels.

capability of gelatin, some other drawbacks, such as low mechanical properties and water sensitivity, limited its potential applications.

Incorporating inorganic nanofillers, such as montmorillonite (MMT), into polymer-based aerogels is an appealing way to increase their performance.[8] MMT clay forms exfoliated gels in water that are rearranged into a house-of-cards structure after freezing. If the process combines clay with a soluble polymer, networks between MMT and polymer chains can be formed, enhancing mechanical and thermal performance.[9] Following this idea, Li et al.[10] have introduced layered double hydroxide particles modified with a silane coupling into an aerogel using glutaraldehyde as a crosslinker. Their results indicated an increase in the mechanical properties, as well as in the thermal conductivity, which reached values between 0.034 and 0.037 W/mK, comparable to that of conventional polystyrene foams (0.033−0.064 W/mK). Zhu and co-workers[11] have prepared an organic−inorganic composite aerogel based on functionalized attapulgite and gelatin through chemical cross-linking and freeze-drying. The improved mechanical and thermal properties were attributed to the good dispersion and excellent assembly of the treated attapulgite nano-rods into the gelatin matrix forming a micro/nano honeycomb like structure. In a different approach, Wang et al.[12] have used gelatin (9−16 wt %) as the mechanical reinforcement and flame retardant agent in polyvinyl alcohol/clay aerogels. While the reduction in flammability was moderate, the compressive modulus was nearly triple that of the aerogel without gelatin. This effect was attributed to the variation in the aerogel microstructure due to the increased hydrogen bonding interactions which changed from a layered to a co-continuous structure.

Another way to enhance aerogel properties is to induce cross-linking of the polymer by a chemical reaction. Among the possibilities, polyphenols are known to react with the amino groups of proteins under oxidative conditions, forming C−N covalent bonds as crosslinks in the gelatin matrix.[13] Tannic acid (TA) is a natural polyphenol compound containing five digallic acids connected through ester linkages to a central glucose core. TA is known to react with proteins via hydrogen bonding, electrostatic bonds, coordination bonding, and hydrophobic interactions.[14,15] Hydrogen bonding can also occur between the carboxylic and amino groups of gelatin and the hydroxyl groups of TA. However, grafting and branching reactions of TA hydroxyls with the gelatin amino groups can considerably modify the raw properties of gelatin.[16,17] Finally, during the combustion process, the tannins form aromatic structures such as graphite−carbon layers that are poor conductors of heat and, therefore, can be used to protect against fire.[18]

Gelatin and gelatin-based hydrogels have been studied extensively, mainly for pharmaceutical or medical applications.[19,20] In addition, enhancing the mechanical properties of the hydrogels through cross-linking has also been the object of considerable research efforts.[21] Regarding gelatin-based aerogels, previous works have mainly focused on selective adsorption of contaminants,[22] wound healing,[23] and drug delivery,[24] among others. However, few works have considered gelatin-based aerogels as structural materials suitable for engineering applications,[3,10,11,25] and to the best of our knowledge, the effect of TA as a crosslinker in gelatin/clay aerogels is described herein for the first time.

https://doi.org/10.1021/acsapm.3c00971
ACS Appl. Polym. Mater. 2023, 5, 7774−7785

Considering the above, this research aimed to produce mechanically robust bio-aerogels with gelatin as the main natural polymer, montmorillonite as a mechanical reinforcement agent, and tannic acid as a natural cross-linking and flame-retardant agent. Such gelatin/tannic acid/clay nanocomposite aerogels were more robust than unmodified gelatin and gelatin/clay aerogels and exhibited enhanced resistance to fire. Moreover, simple dip-coating with polydimethylsiloxane and amino-treated SiO_2 nanoparticles provided superhydrophobicity to the samples, which is necessary for long-lasting applications. The structure and the relevant properties of the formed aerogels were determined and are reported herein.

2. EXPERIMENTAL SECTION

2.1. Materials. Gelatin (G) powder type B, 220−240 Bloom, was purchased from Boter (Badalona, Barcelona, Spain). TA powder was obtained from Merck (Mollet del Vallès, Barcelona, Spain). Sodium montmorillonite clay (C), (PGW grade, ρ = 2.6 g/cm^3) was obtained from Nanocor (Hoffman Estates, Illinois, USA). Sodium hydroxide was supplied by Riser (Les Franqueses del Vallès, Barcelona, Spain).

2.2. Aerogel Preparation. The gel precursors were prepared as follows (Figure 1a): 5 g of gelatin and 5 g of montmorillonite (MMT) clay were separately dispersed in 40 mL of DI water by magnetic stirring, and the respective grams of TA powder was dissolved in 20 mL of DI water. The NaOH solution (34 g/100 mL) was slowly added dropwise into the gelatin and TA solutions until a pH of 10 was reached, measured by pH meter (VWR, Llinars del Vallès, Barcelona, Spain). The MMT clay dispersion was then incorporated in the TA−gelatin blend and stirred using a IKA T-25 Ultra-Turrax disperser at 9000 rpm for 20 min at 60 °C to homogenize the mixture. The final solutions were poured into cylindrical molds (d = 30 mm, h = 25 mm) and square molds (100 × 100 × ∼10 mm) and left to age for 3 h. The aged samples were then frozen in a dry ice/ethanol bath and freeze-dried at −80 °C and 0.02 mbar (Figure 1b) in a lyophilizer (Telstar, Terrassa, Barcelona, Spain). The samples are named for their components and the amount in 100 mL of aqueous solution (Table S1). For instance, G5C5T1 refers to a sample containing 5 g of gelatin, 5 g of clay, and 1 g of TA dissolved in 100 mL of DI water.

The hydrophobization of the aerogel was performed by immersion. 4 g of polydimethylsiloxane (PDMS) along with the hardener (1:10) and 0.5 g of amino-treated SiO_2 nanoparticles were added to 100 mL of tetrahydrofuran (THF) and magnetically stirred for 30 min at 60 °C. The aerogels were left for 30 min, washed, and dried in a vacuum oven for 1 h at 70 °C to remove any trace of solvent.

2.3. Characterization. The molecular weight of the gelatin was obtained from the intrinsic viscosity calculation using an Ubbelohde Type 1B glass capillary viscometer and viscosimeter precision bath VB-1423 (J.P. Selecta, Abrera, Barcelona, Spain) at 37.5 °C. The influence of the pH on the stability of the precursor gels was investigated by measuring the zeta potential in triplicate using a 90Plus Zeta Nanobrook zeta potential analyzer (Brookhaven, NY, USA). The Fourier transform infrared (FTIR) spectra were recorded using a Nicolet 6700 spectrophotometer with a resolution of 1 cm^{-1} (Thermo Fisher Scientific, Waltham, MA, USA) in the attenuated total reflectance mode. Dynamic rheological measurements were performed at room temperature using an AR-G2 rheometer (TA Instruments, New Castle, DE, USA) in a parallel plate (40 mm) configuration under an N_2 atmosphere and with a constant gap of 1 mm. The limits of the linear viscoelastic region were determined by a preset constant strain of 1%. The angular frequency range selected was 0.1 < ω < 100 rad·s^{-1}.

Because moisture may affect the properties of the aerogels, all samples were stabilized at 50% relative humidity for 8 days prior to testing. The bulk density (ρ_b) of the samples was determined by dividing the mass of each aerogel by its volume and averaging the values determined from five samples of each composition. The total porosity was determined using an AccuPyc 1330 helium pycnometer (Micromeritics, Barcelona, Spain). Duplicate measurements were performed.

The morphological microstructure and clay dispersion were observed using a scanning electron microscope (Jeol 7001F, Akishima, Tokyo, Japan) with energy-dispersive X-ray spectroscopy (EDS). X-ray microtomography (μ-CT) images were obtained using a Skyscan 1272 MP (Bruker, MA, USA) with a source voltage and current of 40 kV and 200 μA, respectively, with an exposure time of 1.5 s and an image pixel size of 0.8 μm. The mechanical resistance was studied in the compression mode using a universal testing machine (ZwickRoell Z010, Sant Cugat del Vallès, Barcelona, Spain) with a load cell of 10 kN and a 1 mm/min crosshead rate. A minimum of five specimens of each composition were tested. To determine the total water content, samples were placed in an HE53 moisture-loss analyzer (Mettler Toledo, Columbus, OH, USA) operating at 160 °C with a testing time of 30 min. The reported results are the average of three replicants. A hot disk analyzer was used to measure the thermal conductivity (λ) and effusivity (e) of the aerogels based on the modified transient plane source (TPS) (C-Therm, TCi Thermal Conductivity Analyzer, Fredericton, NB, Canada). The tests were done on cylindrical samples previously flattened by polishing. Each test provided a minimum of seven measurements of thermal conductivity. The specific calorific heat capacity (C_p) and diffusivity (α) were calculated using the following equations

$$C_p = \frac{e^2}{\lambda \rho_b} \tag{1}$$

$$\alpha = \frac{\lambda}{\rho_b C_p} \tag{2}$$

where λ is defined as the transport of energy through the unit-cross-section of a material due to a temperature gradient, e is the rate at a material can absorb heat from surroundings, C_p is the quantity of heat required to rise by one Celsius degree 1 g of a material, and α is the rate of transfer of heat of a material from the hot side to the cold side.

The thermal stability analysis of the aerogels was done in a Mettler Toledo TGA/DSC 1 instrument (Mettler Toledo, Columbus, OH, USA). The samples (∼10 mg) were placed on aluminum pans and heated at 10 °C/min from 30 to 600 °C under a dry nitrogen atmosphere. The combustion behavior was evaluated in an Ineltec BECC cone calorimeter (Tona, Barcelona, Spain) following ISO 5660. Square samples of 100 × 100 × ∼10 mm were exposed to an external heat flux of 50 kW·m^{-2}. Due to the relatively large dimensions of the specimens, only two samples per composition were tested. When the difference between the values of the two initial samples exceeded 10%, a third specimen was tested.

The water contact angle was measured using an optical contact angle system (OCA) (Data Physics, Riverside, CA, USA) using a 3 μL drop of distilled water. A total of five contact angle measurements were made for each sample.

3. RESULTS AND DISCUSSION

3.1. Gelatin Molecular Weight. In the aerogel nomenclature used, the different components are referred to as G for gelatin, T for TA, and C for clay. For example, the aerogel named "G5C5T4" contains 5 g of gelatin, 5 g of clay, and 4 g of TA in 100 mL of DI water to form the precursor hydrogel.

The relative viscosity and intrinsic viscosity [η] were calculated from the efflux times of three different gelatin concentrations, 0.1, 0.46, and 0.7 g/100 mL. The molecular weight was calculated by applying the Mark−Houwink−Sakurada equation

$$[\eta] = k(M_w)^a \tag{3}$$

where M_w is the molecular weight, and k and a are the Mark−Houwink−Sakurada parameters, which were found to be k =

https://doi.org/10.1021/acsapm.3c00971
ACS Appl. Polym. Mater. 2023, 5, 7774−7785

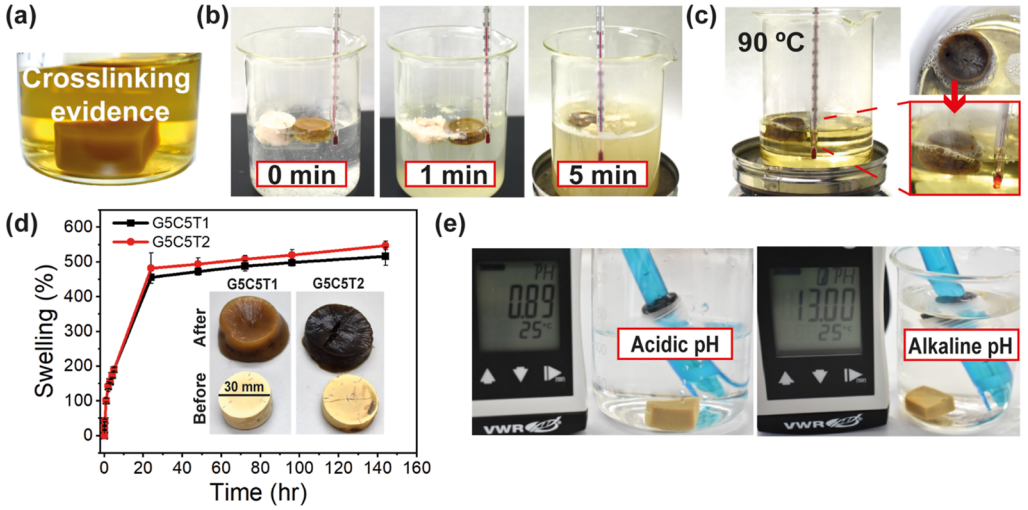

Figure 2. (a) G5C5T1 sample submerged in water, (b) G5 and G5C5T1 aerogels submerged in hot water (60 °C), (c) G5C5T1 aerogel submerged in boiling water, (d) swelling behavior of G5C5T1 and G5C5T2 before and after being submerged in hot water, and (e) G5C5T1 at acidic and alkaline pH.

0.1614 cm^3/g and a = 0.8198, yielding an intrinsic viscosity of $[\eta]$ = 29.03 cm^3/g and a molecular weight of Mw = 563.2 g/mol. The molecular weight of this gelatin is similar to the one reported by Masuelli and Sansone.[26]

3.2. Zeta Potential of Hydrogel Precursors. The zeta potential (ζ) was used to determine the optimal pH for preparing precursor hydrogels. The zeta potentials of two representative gels, G5C5 and G5C5T1, were measured at pH 6 and 10. The zeta potentials obtained under these acidic conditions (−20.61 ± 0.96 and −25.95 ± 0.42 mV, for G5C5 and G5C5T1, respectively) indicated limited stability as a result of low electrostatic repulsion between the different components of the gel. In acidic conditions, the clay edges are positively charged due to H^+ adsorption,[27,28] gelatin has positive and negative charges,[29] and TA is negatively charged. This combination facilitates particle agglomeration and flocculation.

In contrast, a displacement to more negative values (−38.79 ± 0.56 mV for G5C5 and −43.41 ± 0.57 mV for G5C5T1) was found when the pH was 10 (Figure S1), implying more stable solutions.[13] Under alkaline conditions, ζ presented good stability (lower than −30 mV) because the clay absorbed the OH^- ions onto its positive sites, resulting in a global negative charge.[30] Gelatin, an amphiprotic protein, behaved as an anion, while TA was highly dissociated, carrying approximately four negative charges per unit.[31] All these negative charges increased the electrostatic repulsion between the components, making the hydrogel a stable complex and avoiding particle aggregation.

In addition to adding stability to the hydrogels, NaOH was added to promote cross-linking between the gelatin chains and the TA. This process has previously been performed in hydrogels under highly oxidative conditions due to exposure to bubbling oxygen[32] using $NaIO_4$[15,33] or other chemicals.[34]

3.3. Structural Characterization. The FTIR spectra of three representative aerogel compositions are shown in Figure 1c. For clarity, the compositions were selected to best display the structural changes. The FTIR spectra of all aerogels are presented in Figure S2, and the chemical structures of the different compounds are shown in Scheme S1.

The absorption spectrum of gelatin shows bands at 3301−3069, 2937, 1651, 1546, and 1239 cm^{-1}, corresponding to amides A, B, I, II, and III, respectively. Amide A is associated with the stretching vibration of hydrogen-bonded N−H groups. Amide B is associated with the stretching vibration of N−H groups coupled to C−H groups. The amide I and II bands are the major bands of the protein infrared spectrum. Amide I originates from C═O and C−N stretching vibrations and is related to the conformational shifts of the triple helix. Amide II is associated with the in-plane N−H bending and C−N stretching vibrations. Amide III is associated with C−N stretching, N−H bending, C−O bending, and C−C stretching vibrations.[35−37]

After adding MMT clay to the gelatin (G5C5), the spectrum showed new vibrational bands corresponding to Na-MMT clay. The band at 3618 cm^{-1} is due to Al−OH and Si−OH vibrations, the Si−O stretching vibration appears at 1034 cm^{-1}, and the band at 917 cm^{-1} corresponds to the Al_2OH bending vibration. Three peaks located at 623, 520, and 461 cm^{-1} correspond to Mg−O−Si, Al−O−Si, and Si−O−Si bending vibrations, respectively. A slight shift of the amide I and II bands suggests a hydrogen bonding interaction between −OH (at 1648 and 1533 cm^{-1}) from MMT clay and $-COO^-$ and N−H corresponding to gelatin.[9]

In regards to TA, the stretching vibration of the hydroxyl groups from the polyphenols of TA overlaps with amide A in the region between 3700 and 3000 cm^{-1}, whereas the band assigned to CH_2 stretching vibrations overlaps with the absorption band of amide B at ∼2950 cm^{-1}. When 1 g of TA was added to the G5C5 sample, the amide I band shifted from ∼1648 to ∼1651 cm^{-1}. This effect was more pronounced in the G5C5T4 sample (Figure 1c). In this case, the signal intensity increased with a displacement of the amide I band from ∼1651 to ∼1660 cm^{-1} and a shift of the amide II band from ∼1539 to ∼1526 cm^{-1} was also observed. These shifts were attributed to the formation of new C−N covalent bonds from the Schiff base and Michael addition reactions of the quinones obtained by ambient oxidation of the phenol hydroxyl group with the nucleophilic $-NH_2$ groups of gelatin[13,38] (Scheme S2). This band displacement also indicates a significant loss of molecular order and structural

https://doi.org/10.1021/acsapm.3c00971
ACS Appl. Polym. Mater. 2023, 5, 7774−7785

changes in the gelatin, from helical to random coil, due to cross-linking,[39] resulting in insoluble aerogels (Figure 2a). Finally, a significant increase in the intensity of the bands at 1349 and 1198 cm^{-1} was observed in the G5C5T3 and G5C5T4 samples and attributed to asymmetric C−C−O stretching and aromatic C−H deformation due to an excess of TA.

Another technique employed to assess the effect of TA on the gelatin/clay systems is the analysis of the rheology of the hydrogels. In Figure S3, the characteristic parameters, that is, the complex modulus (G^*), storage modulus (G'), the loss modulus (G''), and the complex viscosity (η^*), are plotted as a function of the angular frequency (ω). The relationships between these parameters are defined in the following equations

$$\eta^* = \frac{G'}{\omega} \tag{4}$$

$$G^* = G' + iG'' \tag{5}$$

Two samples with and without TA were compared. TA easily dissolves in water, showing a negligible contribution to the viscosity of the dissolution. However, when TA was added to a gelatin/clay alkaline solution, the complex viscosity and the storage modulus increased by 2 orders of magnitude. An order of magnitude increase in the loss modulus was also detected. In the studied frequency range, the systems behave like stable viscoelastic solids typical of rigid gels. The significant increase in both η^* and G' is attributed to covalent bonding between the gelatin and the TA.

Besides FTIR spectroscopy and rheology, cross-linking between gelatin and TA was also verified by immersing representative aerogels without and with a minimum amount of tannic acid (G5, G5C5T1, and G5C5T2) in different media. The G5 sample dissolved completely in water at 60 °C, whereas G5C5T1 did not dissolve (Figure 2b), even after 30 min of immersion in boiling water (Figure 2c).

However, because of their hydrophilic character, the aerogels swell. For this reason, the swelling behavior of the G5C5T1 and G5C5T2 compositions was monitored with time, and the swelling ratio was calculated as follows

$$S_w\ (\%) = \frac{w_2 - w_1}{w_1} \times 100 \tag{6}$$

where w_1 is the weight of the dried sample, and w_2 is the weight of the sample after immersion. Figure 2d shows the aerogel before and after 140 h of immersion in water and the evolution of the swelling ratio, which reached saturation (S_w = 450−500%) after 24 h.

Finally, the G5C5T1 sample was also introduced into highly acidic and basic solutions to further assess the stability of the TA-modified aerogels. Apart from the aforementioned swelling, no other changes were detected after 48 h of immersion in these media (Figure 2e). Thus, TA is an effective cross-linking agent for gelatin molecules, creating a strong and stable aerogel skeleton.

3.4. Physical Properties. The moisture absorbed by the aerogels was determined after the samples were lyophilized and stabilized at 50% RH until they reached a constant weight; these conditions are similar to the ones expected in applications. The total free and bonded water content was also determined by heating three replicas of each composition to 160 °C for 30 min. The results showed the maximum amount for net gelatin and the minimum for the gelatin/clay aerogel. The values increased with the TA content of the blends (Table 1 and Figure S4).

Table 1. Physical Properties of Aerogels

sample	ρ_b (g/cm^3)	porosity (%)	water content (%)
G5	0.070 ± 0.001	95.1 ± 0.20	17.2 ± 0.4
G5C5	0.098 ± 0.005	94.9 ± 0.18	9.3 ± 0.3
G5C5T1	0.114 ± 0.003	94.3 ± 0.08	12.5 ± 0.4
G5C5T2	0.130 ± 0.002	92.9 ± 0.10	14.7 ± 0.3
G5C5T3	0.155 ± 0.005	91.9 ± 0.05	14.7 ± 0.2
G5C5T4	0.158 ± 0.005	91.4 ± 0.90	15.0 ± 0.3

As expected, the pure gelatin aerogel showed the maximum amount of absorbed moisture among the samples. In contrast, the G5C5 sample had the minimum absorbed moisture due to the physical barrier effect of the clay. The high polarity of TA caused an increase in moisture proportional to the amount of added TA, increasing from G5C5T1 to G5C5T4. Despite this effect, the gelatin composite aerogels containing TA showed lower moisture absorption values than the G5 sample. This behavior is attributed to the hydrogen bonds and formation of crosslinks that reduced the number of free polar groups exposed to the environment.

The bulk densities (ρ_b) of the aerogels increased after adding clay and TA. This increase was expected due to the incorporation of the denser solids, clay (2.6 g/cm^3) and TA (1.56 g/cm^3), into the aerogel structure. The total porosity decreased due to the cross-linking between gelatin and TA, and the higher amount of solids reduced the volumetric expansion of ice during freezing.

3.5. Morphology. The structure of the precursor hydrogels governs the aerogel morphology, which in turn strongly affects the final properties. The main factors are the processing rate (stirring speed), aging time, viscosity, and molecular weight.[40] In this work, a high stirring speed was applied while preparing the precursor gels, which dispersed the clay particles well and ensured a more uniform coating by the matrix. It has been reported that long standing times in the precursor gels can increase the mechanical properties of the corresponding aerogels. Here, a relatively short aging time of 3 h was selected. This short aging time avoided the formation of gradients of clay concentration due to gravity-driven sedimentation.

The micro-CT images of gelatin aerogels are shown in Figure 3a. The 3D general view corresponding to the center of the cylindrical aerogel monolith is shown on the left side. The cross-sections through the $X-Z$ and $X-Y$ planes show a structure with radial orientation due to the forces generated by ice growth. The cross-section through the $Z-Y$ plane shows the front view of the porous distribution, which corresponds to the holes left by the sublimation of ice. These images confirm that ice growth drove the structure of the aerogel during immersion in the −80 °C bath. Ice growth occurred from the cooled surface of the circular molds to the center, the last zone to be frozen.

The microstructures of the cryo-fractured aerogel surfaces imaged by SEM are shown in Figure 3b. Pure gelatin exhibited a pore size below 50 μm. The gelatin precursor hydrogel offered little resistance to ice growth, yielding an irregular open porous structure that tended to collapse due to the low resistance of the gelatin matrix. With the introduction of clay,

https://doi.org/10.1021/acsapm.3c00971
ACS Appl. Polym. Mater. 2023, 5, 7774−7785

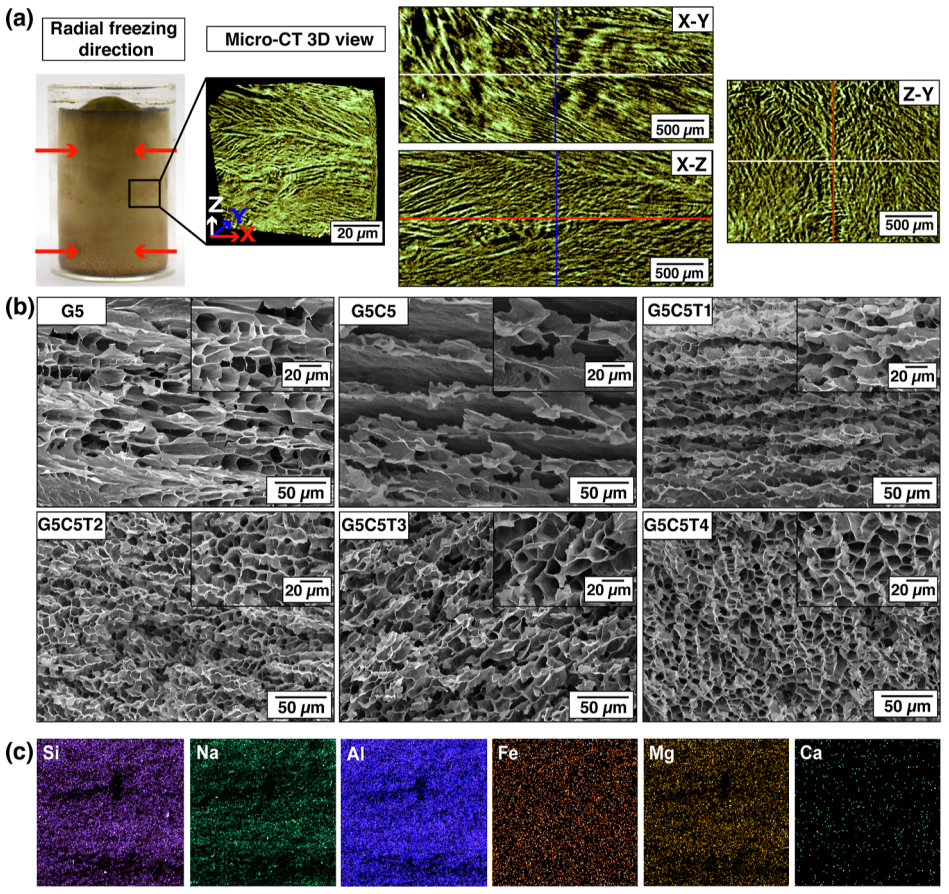

Figure 3. (a) 3D Micro-CT image of the gelatin aerogel structure, (b) SEM microstructure of pure and composite gelatin aerogels, and (c) EDS dispersion of MMT clay performed on the G5C5T3 aerogel.

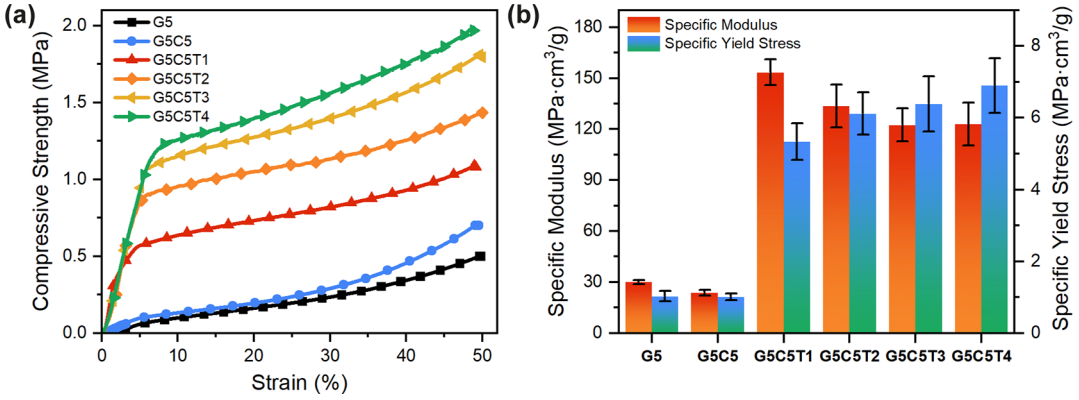

Figure 4. (a) Stress–strain compressive plots of gelatin–clay–TA aerogels and (b) specific modulus and specific yield stress of aerogels studied.

the structure changed into a layered one, in which the gelatin semi-encapsulated the clay. The addition of TA markedly changed the structure: it became more uniform and evolved into a three-dimensional honeycomb-like network. These changes could be due to the increased viscosity from the solid content that hinders ice growth,[41] but they are mainly attributed to the strong attraction between gelatin and tannic acid. Although the density of the honeycomb slightly increased, adding more TA (G5C5T3 and G5C5T4 aerogels) did not substantially affect the microstructure or the MMT dispersion, as can be observed in Figure 3c.

3.6. Compressive Behavior. The gelatin aerogel showed the typical elastoplastic behavior of soft foam (Figure 4a). At low deformation levels (approximately <5%), a linear elastic trend was observed, followed by a plateau at intermediate levels of stress in which the wall of the pores bent and later collapsed, and, finally, the sample densified at the highest applied stresses. The values of the mechanical parameters defining the behavior of the aerogels are presented in Table S2. Adding clay slightly increased Young's modulus from 2.1 to 2.4 MPa and the yield strength from 0.07 to 0.1 MPa (Figure 4b) because the clay–gelatin interaction was only electrostatic.

The excellent dispersion of the MMT filler in the aerogels strengthened the structure and hindered the free deformation of the gelatin chains. Although the influence of the amount of clay was not in the scope of the present research, aerogel

https://doi.org/10.1021/acsapm.3c00971
ACS Appl. Polym. Mater. 2023, 5, 7774–7785

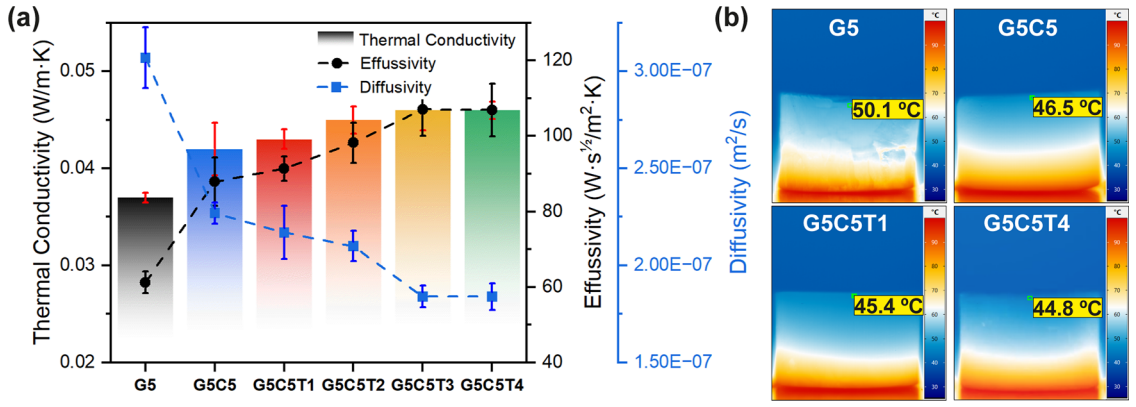

Figure 5. (a) Thermal conductivity, effusivity, and diffusivity and (b) thermographic images of gelatin and gelatin composite aerogels in the axial direction on a hot plate surface at 100 °C.

compressive modulus has been reported to increase monotonically with the clay content.[42] Simultaneously, the stress at yield also increased. However, the incorporation of clay notably increased the viscosity of the precursor gels, making it difficult to manufacture. A clay content of 5 wt % was the maximum possible amount that allowed both good clay dispersion with a suitable gel viscosity.

Introducing TA modified the mechanical performance of the aerogels substantially, transforming them from soft to highly rigid foams. A similar trend has been reported by Li et al. in gelatin/layered double hydroxide-coated particles crosslinked with glutaraldehyde.[10] In the absence of TA, the clay sheets can be clearly seen (see G5C5 in Figure 3b). However, the clay can hardly be seen in the SEM images of the compositions containing TA. It is hypothesized that the clay particles are encapsulated and confined within gelatin−TA chains, acting as short fibers and contributing to the observed increase in mechanical properties.

When the TA content was about 9 wt % (G5C5T1), the compressive modulus increased eight-fold, reaching 18.1 MPa, and the yield stress increased six-fold. The elastic modulus increased marginally at the higher TA contents, reaching its maximum in the G5C5T4 aerogel. Likewise, the energy absorbed during compression increased as more TA was added. This is attributed to the honeycomb structure generated by the gelatin−TA linkage, compared to the layered structure formed by the gelatin−clay. The highest TA concentration introduced brittleness, a typical effect for crosslinked polymer materials. Zhang et al.[16] have reported a decrease in mechanical properties when TA was in excess, attributed to the dual role of TA as a crosslinker and plasticizing agent. In this work, there was neither a decrease in the yield stress nor in Young's modulus, which, together with the increase in brittleness of samples, indicates cross-linking density increasing with TA.

The specific moduli obtained for G5C5T1 and G5C5T2 (153.4 and 133.6 MPa·cm^3/g, respectively) indicated that 1 and 2 g of added TA are appropriate to achieve satisfactory compressive performance, representing a five-fold increase over pure gelatin. Higher values of the specific compressive modulus, 330 MPa·cm^3/g, have been found when phytic acid salt and MMT were incorporated into a gelatin type A matrix, resulting in a two-fold increase compared to that of pure gelatin.[3]

Combining surface-treated attapulgite and gelatin, Zhu et al.[11] have reported specific values of the compressive modulus of the aerogels, 63 MPa·cm^3/g, representing a six-fold increase as compared to pristine gelatin aerogel. In contrast, Li et al. have used layered double hydroxide particles as a reinforcement and glutaraldehyde as a gelatin cross-linking agent. They found a 12-fold increase in the specific modulus of the gelatin, which reached a maximum value of 194 MPa·cm^3/g.[10] Finally, Wang et al. have built a three-dimensional crosslinked polymer aerogel consisting of gelatin, phytic acid, and melamine−formaldehyde, which exhibited high compressive strength (1.98 MPa) and a self-intumescent response when exposed to fire.[43]

The compression testing direction is transverse to the main orientation of the polymer and clay particles, so it yielded relatively low values of the mechanical parameters compared with the radial direction. A representative image of G5C5T4 aerogel loaded with 10 kg is shown in Figure S5. According to the stress−strain curves (Figure 4a), the G5C5T4 aerogel exhibited yield stress of about 1 MPa. For a specimen such as that shown in Figure S4 of 30 mm diameter (transverse surface of 706 mm^2) and 1.68 g weight, this measurement implies it can withstand a maximum total force of 700 N (or 70 kg) without permanent deformation.

3.7. Thermal Conductivity. The thermal insulation properties of the gelatin−clay−TA aerogels were determined by analyzing aerogels through the longitudinal direction by the modified TPS technique. Table S3 shows the thermal conductivities (λ) of aerogels, their effusivity (e), which describes the ability of the material to exchange thermal energy with its surroundings, the specific heat capacity (C_p), and the diffusivity (α), which determines the speed at which thermal equilibrium is reached. The thermal conductivity of the pure gelatin was the lowest, with an average value of 0.037 W/m·K. This is consistent with previous results for similar polymer/clay systems.[44] Although the size of the pores left by the ice was relatively large, the high porosity limited heat transport between the aerogel surfaces over a long distance, keeping thermal conductivity relatively low. As expected, when the clay was introduced, the thermal conductivity increased (∼13%), and the effusivity also rose due to the high intrinsic thermal conductivity of the inorganic clay (Figure 5a). Adding TA also increased both parameters. This effect resulted from the reduced porosity due to the closer connections between the chains caused by gelatin−TA cross-linking.

Regarding C_p, the G5C5 sample had the highest value (1.88 kJ/kg·K), influenced mainly by the percentage of clay in the aerogel structure. After increasing the amount of TA, the C_p of

https://doi.org/10.1021/acsapm.3c00971
ACS Appl. Polym. Mater. 2023, 5, 7774−7785

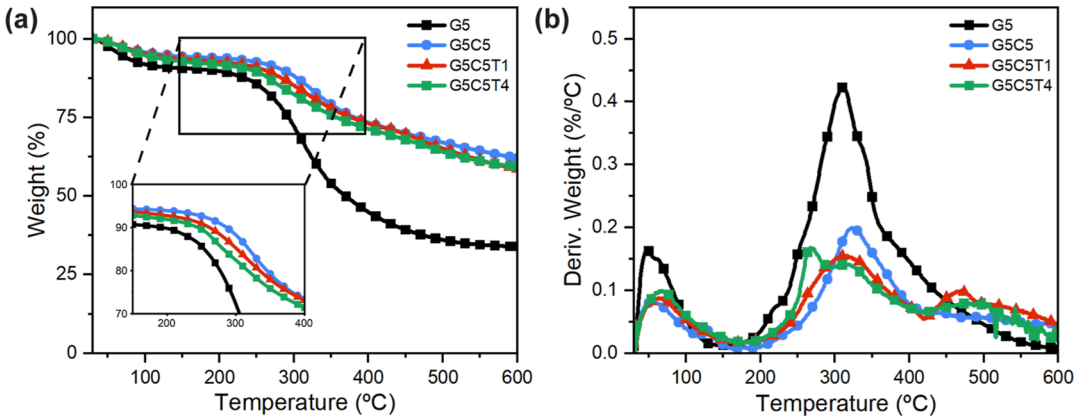

Figure 6. (a) TGA weight loss and (b) derivative thermogravimetric curves of gelatin composite aerogels.

the aerogel composites decreased by ∼19% for sample G5C5T4: less energy was required to increase the temperature of the material. The reduction of diffusivity (Figure 5a) in samples modified by clay and TA means that heat moved more slowly through the aerogel composite skeleton than through that of the pure gelatin. The latter was also evidenced by thermography (Figure 5b). Aerogels were placed on a hot plate at a steady state temperature of 100 °C (Movies S1, S2, S3, and S4). After 20 min of heating, the equilibrium temperatures at the top surface of the aerogels were about 45 °C, indicating that the porous structure of aerogels decreased heat conduction and provided excellent thermal insulation.

3.8. Thermal Stability. The thermal stability of the different aerogels was analyzed using TGA. Figure 6 shows the thermogravimetric curves, and Table S4 summarizes the results, that is, the onset temperature of thermal decomposition (T_{onset}) determined at 5% weight loss after water evaporation, the maximum weight loss rate (dW/dT), the maximum decomposition temperature (Td_{max}), and the residual weight at 600 °C (W_R).

As seen in Figure 6a, the first degradation step below 150 °C was attributed to water loss. The second step occurred between T_{onset} and 400 °C. In this step, the gelatin decomposed rapidly, associated with breaking the triple helix and peptide bonds.[45] When the clay was added (G5C5), a significant decrease in the degradation slope was observed due to the shielding effect. The presence of TA initially helped flatten the degradation slope, possibly due to a combination of water loss and the formation of stable charred compounds. In addition, breaking the TA−gelatin bonds requires more energy, increasing thermal stability. This effect is better distinguished in the derivative curves (Figure 6b). The lowest dW/dT (0.14%/°C) was obtained in the sample containing 2 g of TA (G5C5T2). However, above this amount of TA, the degradation accelerated due to unreacted TA, as observed in the FTIR spectra of G5C5T3 and G5C5T4. The residual weight obtained from the gelatin aerogel composites was nearly double that of pure gelatin aerogel, demonstrating the generation of a stable char layer from clay and TA.

3.9. Fire Behavior. The flame retardancy of the aerogels was first qualitatively tested by Bunsen vertical burning. The flame behavior of pure gelatin and gelatin-modified aerogel is compared in Figure 7a. Pure gelatin aerogel emitted a vigorous flame in the first few seconds and rapidly lost its structural integrity. In contrast, the gelatin composite aerogels kept their shape even after 6 min in contact with the torch (Figure 7b). The aerogels are categorized as self-extinguishing because they did not continue burning when the flame was removed (Movies S5 and S6).

A cone calorimeter was used to quantitatively evaluate the combustion behavior properties of the aerogels as it shows a good correlation between laboratory-scale experiments and an actual fire scenario. The tests were done at a heat flux of 50 kW/m^2, corresponding to the flux found in a developing fire. The main parameters, which are the time to ignition (TTI), the peak of heat release (PHRR), the time to peak of heat release (TTPHRR), and the total heat release (THR), are listed in Table 2. In addition, the fire growth (FIGRA) index, the ratio between PHRR and HRR, the fire performance index (FPI), and the ratio between TTI and PHRR were used to compare the different aerogel compositions. FIGRA and FPI are two critical parameters for the characterization of fire safety. A low FIGRA or a high FPI indicates a low risk from a potential fire. MARHE is the maximum average heat rate emission, a parameter that ranks the ability of materials to suppress flame spread and prevent propagation to other objects.[53] As shown in Figure 7c, unmodified gelatin immediately burned, while adding clay and TA helped retard the TTI. Upon ignition, gelatin showed a fast, vigorous burn with a single peak on the HRR that reached a maximum of 261 kW/m^2 and depended only on the total fuel loading. In contrast, the HRR signals in the modified aerogels had a double-shouldered signal, with the maximum peak decreasing four-fold to reach a minimum value of 64 kW/m^2 in G5C5T1. These curves are characteristics of thermally thick charring materials in which a stable char layer is first formed. The second peak corresponds to the breaking of the char layer or increased pyrolysis.

Higher contents of TA did not further decrease the HRR; on the contrary, the HRR increased in parallel with the THR (Figure 7d). This is attributed to the combustion of pure TA, which reached an HRR peak of 400 kW/m^2 when it was directly exposed to radiation (Figure S6). Accordingly, TA is only effective as a charring agent, provided it is protected from oxygen action. This protection can be reached by adding relatively low contents of TA to the blends. At high contents (G5C5T3 and G5C5T4), free TA migrates toward the surface of the aerogel, contributing to the rise in the HRR. It has been demonstrated that well-distributed inorganic fillers such as clay can significantly enhance the fire retardancy of polymer composites.[54] In the present case, this decrease occurred from the generation of a protective layer on top of the samples

https://doi.org/10.1021/acsapm.3c00971
ACS Appl. Polym. Mater. 2023, 5, 7774−7785

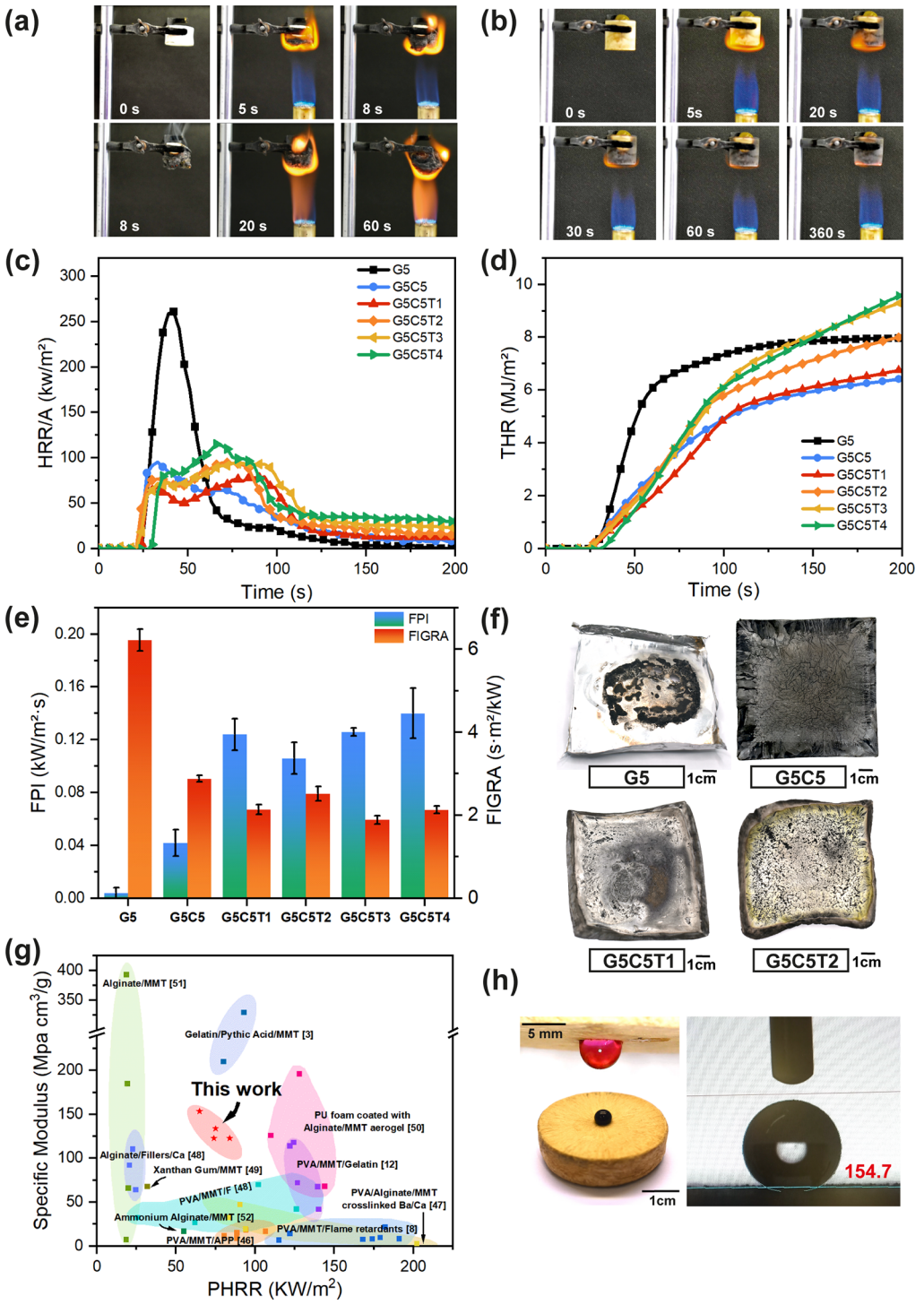

Figure 7. Flame behavior of (a) G5 and (b) G5C5T1 aerogels under Bunsen burner, (c) main representative HRR and (d) THR curves from gelatin aerogel composites, (e) FPI and FIGRA comparison, (f) residue left after combustion, (g) the specific moduli and PHRR of prepared gelatin aerogel composites compared with those of other aerogel clay composites,[3,8,12,46−52] and (h) hydrophobized aerogel upside-down with a water droplet dyed with $KMnO_4$ on the hydrophobized aerogel surface and contact angle measurement.

due to clay platelets re-organizing into a compact network structure. At the early stages of the degradation process, this layer reduced the amount of combustible volatile compounds released, increasing TTI. The clay inhibited TA oxidation in the second stage, allowing its pyrolytic decomposition to carbonaceous structures. The TA decomposition also released bound water that absorbs heat, lowering the temperature of the solid phase and decreasing the PHRR. The final shoulder at long exposure times was due to the material burning at the bottom of the specimens. The generation of small cracks in the brittle carbonized surface allowed oxygen and radiation to contact the underlying material, the burning of which caused the second broad peak in the HRR plot. As shown in Figure 7e, the results of both FPI and FIGRA confirmed that the potential danger from fire notably decreases with the addition of clay and TA.

https://doi.org/10.1021/acsapm.3c00971
ACS Appl. Polym. Mater. 2023, 5, 7774−7785

Table 2. Cone Calorimeter Parameters for the Aerogels in This Study

sample	TTI (s)	PHRR (kW/m^2)	TTPHRR (s)	THR (MJ/m^2)	FPI (kW/m^2·s)	FIGRA (s·m^2/kW)	W_R (%)
G5	1 ± 1	261 ± 0.65	42 ± 2	7.96 ± 0.04	0.004 ± 0.004	6.22 ± 0.26	11.5 ± 0.06
G5C5	4 ± 1	96 ± 1.02	33 ± 1	6.97 ± 1.00	0.042 ± 0.010	2.88 ± 0.08	48.5 ± 2.73
G5C5T1	8 ± 1	65 ± 1.82	30 ± 3	7.63 ± 0.54	0.124 ± 0.012	2.14 ± 0.12	46.7 ± 1.50
G5C5T2	8 ± 1	75 ± 1.41	30 ± 3	8.62 ± 0.96	0.106 ± 0.012	2.52 ± 0.17	48.5 ± 0.80
G5C5T3	9 ± 1	74 ± 1.25	39 ± 3	12.31 ± 0.44	0.126 ± 0.003	1.89 ± 0.10	44.4 ± 0.38
G5C5T4	12 ± 2	84 ± 0.50	39 ± 2	12.72 ± 0.45	0.140 ± 0.019	2.13 ± 0.09	40.6 ± 0.79

Further increases in TA did not enhance the fire resistance of the samples. Although affected by a certain scatter, the MARHE values were reduced by half with the addition of clay. Similar to the HRR, these values increased with the added TA (Figure S7) because of the increased burning mass in the composites. The developed aerogel composites showed an excellent balance between mechanical and fire properties, making them suitable candidates for engineering applications. As expected, the amount of residue left by the aerogels increased with the addition of clay (G5C5), yielding black carbonized ashes and matching the theoretical percentage of clay in the blend well. When additional TA was added, the residual char became a yellowish color due to the thermo-oxidation of the excess TA at the surface of the aerogels (Figure 7f). At the same time, the bulk TA charred, increasing the amount of residue.

Finally, Figure 7g compares the specific moduli and PHRR of our gelatin aerogel composites with those of other relevant polymer−clay aerogels. In general, aerogels in this study presented competitive values compared to those of these similar systems.

3.10. Hydrophobization. Moisture absorption and swelling after prolonged water contact may constitute a significant handicap for future applications of gelatin-based aerogels. However, these drawbacks can be overcome by a simple process, surface hydrophobization.

The hydrophobization was carried out by immersion of the aerogels in a THF solution containing PDMS and SiO_2 nanoparticles. The tetrahydrofuran was used to decrease the viscosity of the PDMS and disperse the nanoparticles. SEM observations of the treated aerogels revealed a coating completely covering the surface (Figure S8) and confirmed the presence of SiO_2 nanoparticles on the surface.

Figure 7h shows images of a water droplet on the G5C5T1 aerogel after surface hydrophobization. The darkish water droplet dyed with $KMnO_4$ remained unaltered on the aerogel surface. In addition, there were good surface adhesion properties as large water droplets did not fall off after the aerogel surface was inverted. The measurement of the water contact angle yielded a value of 154 ± 2°, indicating a superhydrophobic character. The surface energy of the aerogels decreased due to the presence of the hydrophobic groups ($-CH_3$) of PDMS. The combination of the low surface energy of the PDMS coating and the micro-roughness from the SiO_2 nanoparticles achieved superhydrophobicity on the aerogel surfaces, maintaining the thermal insulation and fire resistance properties in ambient humidity.

4. CONCLUSIONS

Mechanically robust and fire-resistant bio-aerogels formed from gelatin, clay, and TA were prepared by a simple freeze-drying process. Aerogels containing different amounts of TA were prepared, and their properties were compared with those of unmodified aerogel. Crosslinked hydrogels were formed under alkaline conditions due to covalent bonding between the gelatin and the TA. These interactions led to stable aerogels suitable for use in harsh environments. The TA-modified aerogels exhibited much higher mechanical performance than those without tannic acid, reaching Young's modulus as high as 19.4 MPa and a 15-fold increase in the stress at yield. The thermal conductivity was maintained in the lower range for this type of aerogel. However, both cross-linking and clay contributed to the increase in the thermal conductivity compared to that of pure gelatin. The protecting action of well-dispersed nano-clay particles promoted the pyrolytic decomposition and charring action of TA, providing the resulting aerogels with excellent flame-retardant capabilities. The hydrophilic character of the aerogels was modified by a simple coating method, which made the surface. The combination of multifunctional properties in these fully bio-based aerogels could expand the applications of these sustainable foam-like materials, which could eventually be used to replace traditional petrol-based foams.

■ ASSOCIATED CONTENT

Supporting Information

The Supporting Information is available free of charge at https://pubs.acs.org/doi/10.1021/acsapm.3c00971.

Thermographic evolution of G5 aerogel on a hot plate surface (AVI)

Thermographic evolution of G5C5 aerogel on a hot plate surface (AVI)

Thermographic evolution of G5C5T1 aerogel on a hot plate surface (AVI)

Thermographic evolution of G5C5T4 aerogel on a hot plate surface (AVI)

Flame behavior of G5 aerogel under a bunsen burner (MP4)

Flame behavior of G5C5T1 aerogel under a bunsen burner (MP4)

Aerogel compositions; mechanical properties of the different aerogel compositions; thermal insulation properties of composite aerogels; thermogravimetric results of composite aerogels; structures of gelatin, tannic acid, and montmorillonite; proposed reaction mechanism between gelatin/tannic acid; zeta potential of two representative hydrogel precursors at acidic (pH 6) and at basic (pH 10) conditions; FTIR spectra of the different aerogel composites; rheology behavior of hydrogels G5C5 and G5C5T2; moisture absorption of aerogel compositions; weight of the G5C5T4 aerogel and its resistant behavior under 10 kg of weight on top; HRR curve of tannic acid powder; THReff and MARHE comparison; and SEM micrographs of G5C5T1 and G5C5T4 aerogel surface after hydrophobization (PDF)

https://doi.org/10.1021/acsapm.3c00971
ACS Appl. Polym. Mater. 2023, 5, 7774−7785

AUTHOR INFORMATION

Corresponding Author

Miguel Sánchez-Soto − *Departament de Ciència I Enginyeria de Materials, Escola d'Enginyeria de Barcelona Est. (EEBE), Universitat Politècnica de Catalunya-Barcelona Tech (UPC), 08019 Barcelona, Spain;* orcid.org/0000-0002-0023-5059; Phone: +34-937398140; Email: m.sanchez-soto@upc.edu

Authors

Lucía G. De la Cruz − *Departament de Ciència I Enginyeria de Materials, Escola d'Enginyeria de Barcelona Est. (EEBE), Universitat Politècnica de Catalunya-Barcelona Tech (UPC), 08019 Barcelona, Spain;* orcid.org/0000-0001-9009-4503

Tobias Abt − *Departament de Ciència I Enginyeria de Materials, Escola d'Enginyeria de Barcelona Est. (EEBE), Universitat Politècnica de Catalunya-Barcelona Tech (UPC), 08019 Barcelona, Spain;* orcid.org/0000-0002-4351-8155

Noel León − *Departament de Ciència I Enginyeria de Materials, Escola d'Enginyeria de Barcelona Est. (EEBE), Universitat Politècnica de Catalunya-Barcelona Tech (UPC), 08019 Barcelona, Spain;* orcid.org/0000-0003-1061-8552

Complete contact information is available at: https://pubs.acs.org/10.1021/acsapm.3c00971

Author Contributions

The manuscript was written through contributions of all authors. All authors have given approval to the final version of the manuscript.

Notes

The authors declare no competing financial interest.

ACKNOWLEDGMENTS

The authors thank the Ministerio de Ciencia e Innovación (Spain) for the funding received for the execution of the project: UpECOBLENDS with reference PID2019-106518RB I00/AEI/10.13039/501100011033. The authors also thank the Generalitat de Catalunya for the grant 2021SGR01042. L.G.D. also thanks the Consejo Nacional de Ciencia y Tecnología, CONAHCYT for the full PhD grant (no. 729201) provided.

REFERENCES

(1) Jiang, S.; Zhang, M.; Li, M.; Zhu, J.; Ge, A.; Liu, L.; Yu, J. Cellulose-Based Composite Thermal-Insulating Foams toward Eco-Friendly, Flexible and Flame-Retardant. *Carbohydr. Polym.* **2021**, *273*, 118544.

(2) Ye, D.-D.; Wang, T.; Liao, W.; Wang, H.; Zhao, H.-B.; Wang, Y.-T.; Xu, S.; Wang, Y.-Z. Ultrahigh-Temperature Insulating and Fire-Resistant Aerogels from Cationic Amylopectin and Clay via a Facile Route. *ACS Sustainable Chem. Eng.* **2019**, *7*, 11582−11592.

(3) Wang, Y.-T.; Zhao, H.-B.; Guo, M.-L.; Degracia, K.; Sun, H.; Sun, M.-Z.; Zhao, Z.-Y.; Schiraldi, D. A.; Wang, Y.-Z. Rigid and Fire-Resistant All-Biomass Aerogels. *ACS Sustainable Chem. Eng.* **2022**, *10*, 12117−12126.

(4) Jin, H.; Zhou, X.; Xu, T.; Dai, C.; Gu, Y.; Yun, S.; Hu, T.; Guan, G.; Chen, J. Ultralight and Hydrophobic Palygorskite-Based Aerogels with Prominent Thermal Insulation and Flame Retardancy. *ACS Appl. Mater. Interfaces* **2020**, *12*, 11815−11824.

(5) De la Cruz, L. G.; Abt, T.; León, N.; Wang, L.; Sánchez-Soto, M. Ice-Template Crosslinked PVA Aerogels Modified with Tannic Acid and Sodium Alginate. *Gels* **2022**, *8*, 419.

(6) Yun, L.; Zhao, J.; Kang, X.; Du, Y.; Yuan, X.; Hou, X. Preparation and Properties of Monolithic and Hydrophobic Gelatin−Silica Composite Aerogels for Oil Absorption. *J. Sol-Gel Sci. Technol.* **2017**, *83*, 197−206.

(7) Zhang, L.; Huang, Y.; Sun, P.; Hai, Y.; Jiang, S. A Self-Healing, Recyclable, and Degradable Fire-Retardant Gelatin-Based Biogel Coating for Green Buildings. *Soft Matter* **2021**, *17*, 5231−5239.

(8) Wang, L.; Sánchez-Soto, M.; Maspoch, M. L. Polymer/Clay Aerogel Composites with Flame Retardant Agents: Mechanical, Thermal and Fire Behavior. *Mater. Des.* **2013**, *52*, 609−614.

(9) Xu, S. W.; Zheng, J. P.; Tong, L.; Yao, K. D. Interaction of Functional Groups of Gelatin and Montmorillonite in Nano-composite. *J. Appl. Polym. Sci.* **2006**, *101*, 1556−1561.

(10) Li, H.; Zhao, F.; Peng, T.; Jiang, C.; Liu, H.; He, Y.; He, D. Robust, Lightweight Gelatin Composite Aerogel with Outstanding Thermal Insulation. *J. Mater. Sci.* **2022**, *57*, 14835−14847.

(11) Zhu, J.; Zhao, F.; Xiong, R.; Peng, T.; Ma, Y.; Hu, J.; Xie, L.; Jiang, C. Thermal Insulation and Flame Retardancy of Attapulgite Reinforced Gelatin-Based Composite Aerogel with Enhanced Strength Properties. *Composites, Part A* **2020**, *138*, 106040.

(12) Wang, Y.-T.; Zhao, H.-B.; Degracia, K.; Han, L.-X.; Sun, H.; Sun, M.; Wang, Y.-Z.; Schiraldi, D. A. Green Approach to Improving the Strength and Flame Retardancy of Poly(Vinyl Alcohol)/Clay Aerogels: Incorporating Biobased Gelatin. *ACS Appl. Mater. Interfaces* **2017**, *9*, 42258−42265.

(13) Zhang, X.; Do, M. D.; Casey, P.; Sulistio, A.; Qiao, G. G.; Lundin, L.; Lillford, P.; Kosaraju, S. Chemical Cross-Linking Gelatin with Natural Phenolic Compounds as Studied by High-Resolution NMR Spectroscopy. *Biomacromolecules* **2010**, *11*, 1125−1132.

(14) Peña, C.; de la Caba, K.; Eceiza, A.; Ruseckaite, R.; Mondragon, I. Enhancing Water Repellence and Mechanical Properties of Gelatin Films by Tannin Addition. *Bioresour. Technol.* **2010**, *101*, 6836−6842.

(15) Zhao, Q.; Mu, S.; Long, Y.; Zhou, J.; Chen, W.; Astruc, D.; Gaidau, C.; Gu, H. Tannin-Tethered Gelatin Hydrogels with Considerable Self-Healing and Adhesive Performances. *Macromol. Mater. Eng.* **2019**, *304*, 1800664.

(16) Zhang, X.; Do, M. D.; Casey, P.; Sulistio, A.; Qiao, G. G.; Lundin, L.; Lillford, P.; Kosaraju, S. Chemical Modification of Gelatin by a Natural Phenolic Cross-Linker, Tannic Acid. *J. Agric. Food Chem.* **2010**, *58*, 6809−6815.

(17) Wu, J.; Liao, W.; Zhang, J.; Chen, W. Microwave-Assisted Reaction of Gelatin with Tannic Acid: Non-Thermal Effect on the Crosslinking Process. *Chem. Eng. Commun.* **2019**, *206*, 1152−1158.

(18) Lang, X.; Shang, K.; Wang, Y.-Z.; Schiraldi, D. A. Low Flammability Foam-like Materials Based on Epoxy, Tannic Acid, and Sodium Montmorillonite Clay. *Green Mater.* **2015**, *3*, 43−51.

(19) Jaipan, P.; Nguyen, A.; Narayan, R. J. Gelatin-Based Hydrogels for Biomedical Applications. *MRS Commun.* **2017**, *7*, 416−426.

(20) Camci-Unal, G.; Cuttica, D.; Annabi, N.; Demarchi, D.; Khademhosseini, A. Synthesis and Characterization of Hybrid Hyaluronic Acid-Gelatin Hydrogels. *Biomacromolecules* **2013**, *14*, 1085−1092.

(21) Tang, L.; Zhang, D.; Gong, L.; Zhang, Y.; Xie, S.; Ren, B.; Liu, Y.; Yang, F.; Zhou, G.; Chang, Y.; Tang, J.; Zheng, J. Double-Network Physical Cross-Linking Strategy To Promote Bulk Mechanical and Surface Adhesive Properties of Hydrogels. *Macromolecules* **2019**, *52*, 9512−9525.

(22) Jiang, J.; Zhang, Q.; Zhan, X.; Chen, F. A Multifunctional Gelatin-Based Aerogel with Superior Pollutants Adsorption, Oil/Water Separation and Photocatalytic Properties. *Chem. Eng. J.* **2019**, *358*, 1539−1551.

(23) Mao, Z.; Bai, J.; Jin, X.; Mao, W.; Dong, Y. Construction of a Multifunctional 3D Nanofiber Aerogel Loaded with ZnO for Wound Healing. *Colloids Surf., B* **2021**, *208*, 112070.

(24) Li, J.; Wang, Y.; Zhang, L.; Xu, Z.; Dai, H.; Wu, W. Nanocellulose/Gelatin Composite Cryogels for Controlled Drug Release. *ACS Sustainable Chem. Eng.* **2019**, *7*, 6381−6389.

(25) Li, S.-L.; Wang, J.; Zhao, H.-B.; Cheng, J.-B.; Zhang, A.-N.; Wang, T.; Cao, M.; Fu, T.; Wang, Y.-Z. Ultralight Biomass Aerogels

with Multifunctionality and Superelasticity Under Extreme Conditions. *ACS Appl. Mater. Interfaces* **2021**, *13*, 59231−59242.
(26) Masuelli, M. A.; Sansone, M. G. Hydrodynamic Properties of Gelatin - Studies from Intrinsic Viscosity Measurements. In *Products and Applications of Biopolymers*; IntechOpen: Rijeka, 2012. Ch. 5. DOI: 10.5772/34401.
(27) Kubilay, Ş.; Gürkan, R.; Savran, A.; Şahan, T. Removal of Cu(II), Zn(II) and Co(II) Ions from Aqueous Solutions by Adsorption onto Natural Bentonite. *Adsorption* **2007**, *13*, 41−51.
(28) Preocanin, T.; Abdelmonem, A. Charging Behavior of Clays and Clay Minerals in Aqueous Electrolyte Solutions — Experimental Methods for Measuring the Charge and Interpreting the Results. In *Clays, Clay Minerals and Ceramic Materials Based on Clay Minerals*; IntechOpen: Rijeka, 2016. Ch. 3. DOI: 10.5772/62082.
(29) Schrieber, R.; Gareis, H. From Collagen to Gelatine. In *Gelatine Handbook*; John Wiley & Sons, Ltd, 2007, pp 45−117. DOI: 10.1002/9783527610969.ch2.
(30) Fil, B. A.; Özmetin, C.; Korkmaz, M. Characterization and Electrokinetic Properties of Montmorillonite. *Bulg. Chem. Commun.* **2014**, *46*, 258−263.
(31) An, J.-H.; Dultz, S. Adsorption of Tannic Acid on Chitosan-Montmorillonite as a Function of PH and Surface Charge Properties. *Appl. Clay Sci.* **2007**, *36*, 256−264.
(32) Strauss, G.; Gibson, S. M. Plant Phenolics as Cross-Linkers of Gelatin Gels and Gelatin-Based Coacervates for Use as Food Ingredients. *Food Hydrocolloids* **2004**, *18*, 81−89.
(33) Zhao, X.; Zhang, M.; Guo, B.; Ma, P. X. Mussel-Inspired Injectable Supramolecular and Covalent Bond Crosslinked Hydrogels with Rapid Self-Healing and Recovery Properties via a Facile Approach under Metal-Free Conditions. *J. Mater. Chem. B* **2016**, *4*, 6644−6651.
(34) Osetrov, K.; Uspenskaya, M.; Sitnikova, V. The Influence of Oxidant on Gelatin−Tannin Hydrogel Properties and Structure for Potential Biomedical Application. *Polymers* **2022**, *14*, 150.
(35) Bandekar, J. Amide Modes and Protein Conformation. *Biochim. Biophys. Acta Protein Struct. Mol. Enzymol.* **1992**, *1120*, 123−143.
(36) Barth, A.; Zscherp, C. What Vibrations Tell about Proteins. *Q. Rev. Biophys.* **2002**, *35*, 369−430.
(37) Ji, Y.; Yang, X.; Ji, Z.; Zhu, L.; Ma, N.; Chen, D.; Jia, X.; Tang, J.; Cao, Y. DFT-Calculated IR Spectrum Amide I, II, and III Band Contributions of N-Methylacetamide Fine Components. *ACS Omega* **2020**, *5*, 8572−8578.
(38) Hagerman, A. E. Chemistry of Tannin-Protein Complexation. In *Chemistry and Significance of Condensed Tannins*; Hemingway, R. W., Karchesy, J. J., Branham, S. J., Eds.; Springer US: Boston, MA, 1989, pp 323−333. DOI: 10.1007/978-1-4684-7511-1_20.
(39) Anvari, M.; Chung, D. Dynamic Rheological and Structural Characterization of Fish Gelatin − Gum Arabic Coacervate Gels Cross-Linked by Tannic Acid. *Food Hydrocolloids* **2016**, *60*, 516−524.
(40) Sun, M.; Sun, H.; Wang, Y.; Sánchez-Soto, M.; Schiraldi, D. A. The Relation between the Rheological Properties of Gels and the Mechanical Properties of Their Corresponding Aerogels. *Gels* **2018**, *4*, 33.
(41) Wang, Y.; Gawryla, M. D.; Schiraldi, D. A. Effects of Freezing Conditions on the Morphology and Mechanical Properties of Clay and Polymer/Clay Aerogels. *J. Appl. Polym. Sci.* **2013**, *129*, 1637−1641.
(42) Chen, H.-B.; Chiou, B.-S.; Wang, Y.-Z.; Schiraldi, D. A. Biodegradable Pectin/Clay Aerogels. *ACS Appl. Mater. Interfaces* **2013**, *5*, 1715−1721.
(43) Wang, T.; Long, M.-C.; Zhao, H.-B.; An, W.-L.; Xu, S.; Deng, C.; Wang, Y.-Z. Temperature-Responsive Intumescent Chemistry toward Fire Resistance and Super Thermal Insulation under Extremely Harsh Conditions. *Chem. Mater.* **2021**, *33*, 6018−6028.
(44) Chen, B.; Zheng, Q.; Zhu, J.; Li, J.; Cai, Z.; Chen, L.; Gong, S. Mechanically Strong Fully Biobased Anisotropic Cellulose Aerogels. *RSC Adv.* **2016**, *6*, 96518−96526.
(45) Weiss, I. M.; Muth, C.; Drumm, R.; Kirchner, H. O. K. Thermal Decomposition of the Amino Acids Glycine, Cysteine, Aspartic Acid, Asparagine, Glutamic Acid, Glutamine, Arginine and Histidine. *BMC Biophys.* **2018**, *11*, 2.
(46) Wang, Y.-T.; Liao, S.-F.; Shang, K.; Chen, M.-J.; Huang, J.-Q.; Wang, Y.-Z.; Schiraldi, D. A. Efficient Approach to Improving the Flame Retardancy of Poly(Vinyl Alcohol)/Clay Aerogels: Incorporating Piperazine-Modified Ammonium Polyphosphate. *ACS Appl. Mater. Interfaces* **2015**, *7*, 1780−1786.
(47) Wu, N.; Niu, F.; Lang, W.; Xia, M. Highly Efficient Flame-Retardant and Low-Smoke-Toxicity Poly(Vinyl Alcohol)/Alginate/Montmorillonite Composite Aerogels by Two-Step Crosslinking Strategy. *Carbohydr. Polym.* **2019**, *221*, 221−230.
(48) Chen, H.-B.; Schiraldi, D. A. Flammability of Polymer/Clay Aerogel Composites: An Overview. *Polym. Rev.* **2019**, *59*, 1−24.
(49) Wang, L.; Schiraldi, D. A.; Sánchez-Soto, M. Foamlike Xanthan Gum/Clay Aerogel Composites and Tailoring Properties by Blending with Agar. *Ind. Eng. Chem. Res.* **2014**, *53*, 7680−7687.
(50) Chen, H.-B.; Shen, P.; Chen, M.-J.; Zhao, H.-B.; Schiraldi, D. A. Highly Efficient Flame Retardant Polyurethane Foam with Alginate/Clay Aerogel Coating. *ACS Appl. Mater. Interfaces* **2016**, *8*, 32557−32564.
(51) Li, X.-L.; Chen, M.-J.; Chen, H.-B. Facile Fabrication of Mechanically-Strong and Flame Retardant Alginate/Clay Aerogels. *Composites, Part B* **2019**, *164*, 18−25.
(52) Chen, H.-B.; Wang, Y.-Z.; Sánchez-Soto, M.; Schiraldi, D. A. Low Flammability, Foam-like Materials Based on Ammonium Alginate and Sodium Montmorillonite Clay. *Polymer* **2012**, *53*, 5825−5831.
(53) *ISO 5660-1 Reaction to Fire Tests - Heat Release, Smoke Production and Mass Loss Rate*, International Organization for Standardization, 2015.
(54) Kashiwagi, T.; Du, F.; Douglas, J. F.; Winey, K. I.; Harris, R. H.; Shields, J. R. Nanoparticle Networks Reduce the Flammability of Polymer Nanocomposites. *Nat. Mater.* **2005**, *4*, 928−933.